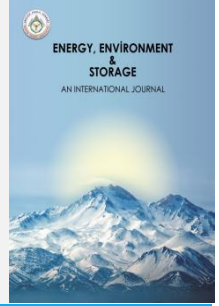




# Energy, Environment and Storage

JournalHomepage: [www.enenstrg.com](http://www.enenstrg.com)



## Experimental and Numerical Analysis of Savonius Wind Turbine with End Plate on Various Types

MahmutBurak Akkus<sup>1\*</sup>, Zeki Haksever<sup>1</sup>, Suleyman Teksin<sup>1,2</sup>

<sup>1</sup>Erciyes University, Faculty of Engineering, Department of Mechanical Engineering, Kayseri, Turkey

<sup>1</sup> [mbakkus54@gmail.com](mailto:mbakkus54@gmail.com), ORCID:0000-0002-4561-7093

<sup>1</sup>Erciyes University, Faculty of Engineering, Department of Mechanical Engineering, Kayseri, Turkey

<sup>1</sup> [zhaksever@gmail.com](mailto:zhaksever@gmail.com), ORCID: 0000-0001-7037-4540

<sup>1,2</sup>Van YuzuncuYil University, Faculty of Engineering, Department of Mechanical Engineering, Van, Turkey

<sup>1,2</sup> [steksin@yyu.edu.tr](mailto:steksin@yyu.edu.tr), [steksin@erciyes.edu.tr](mailto:steksin@erciyes.edu.tr), ORCID:0000-0001-8854-0332

**ABSTRACT.** This study aims to observe whether the overall yield has changed utilizing the different blade structures and the end plates placed on the different blade structures of the Savonius-type wind turbine. End plates of different diameters are placed at the top and bottom of the turbine to increase overall efficiency. While the experimental analysis was conducted in the aerodynamic laboratory of the faculty of Aeronautical and Astronautical at Erciyes University, Ansys Fluent software is used for numerical calculations. The turbine structure used for the numerical study is made according to the optimum values taken from the experimental investigation to minimize the time wasted. The results in the experimental and numerical analysis were compared with each other and the overall yield was observed to increase according to these analysis results. The presence of the end plate significantly increased the efficiency of the savonius turbine and allowed it to operate in the higher *TSR* range. This increase is directly proportional to the enlarging in the diameter of the end plate.

**Keywords:** Efficiency, Turbine, VAWT, Savonius, Numerical-Experimental Analysis

Article History: Received: 02.03.2022; Revised: 04.03.2022; Accepted: 27.04.2022; Available online: 24.05.2022

Doi: <https://doi.org/10.52924/IUIX7477>

### 1. INTRODUCTION

Although fossil fuels are mostly used in energy production in today's energy systems, energy production models are gradually moving to renewable energy. An important reason for this is the increase in prices of fossil resources recently [1]. Especially in the last decade, it became possible to increase the sustainability of energy production systems using the benefits of the newest technologies. For instance, methods of wind power energy systems have become more popular due to being environment-friendly and developing technologies. Furthermore, wind power energy systems generate electrical power through wind turbines. While more electricity can be produced especially from other renewable energy sources. There is no carbon emission in electricity production in wind energy [2]. Even though wind turbines might differ in terms of structure, size, and number of blades, they function in the same manner. The main functionality of wind turbines is to use the airflow within their body as much as possible to convert it into electrical energy.

Although the efficiency of horizontal axis wind turbines is generally higher, vertical axis wind turbines are also widely used due to high installation and maintenance costs, high noise [3], and less wear of the parts in the system. In addition, taking the wind coming on the turbine from all directions is another important advantage and it is independent of the wind direction. Their ability to self-starting at low wind speeds is high [4]. Savonius wind turbines, whose general appearance resembles the letter S, is one of these vertical axis turbine structures.

An increasing number of studies about general structure or optimization are being conducted on wind turbines. Lots of variations affect the performance of the Savonius wind turbine such as blade shape, number of blades, gap ratio, overlap ratio, end plate, etc. [5,6]. Moreover, the wind velocity is also important for increasing the Savonius turbine performance [7].

The overlap ratio is the ratio between the distance of overlap to the turbine diameter. It also decreased the

negative drag [8]. Fujisawa [9] determined the bucket overlap around 15%. Gupta et al. [10] have investigated both the three-bucket Darrieus and Savonius-Darrieus rotor. They found that the combination showed better performance. Simsek et al. [11] studied the different models of Savonius turbine. They used 12 models with 3 different structures by changing the number of blades. According to their study, 3 bladed modified turbine has better performance. Lee and Lim [12] investigated the performance characteristics of helical Savonius. They determined the maximum power coefficient at an angle of 45°. When this angle was set to 90° and 135°, start to decrease for  $C_p$ .

Low aspect ratios are used in designing Savonius rotors to avoid the structural failure problem of rotors due to high aspect ratios [13]. Ushiyama and Nagai [14] recommended the optimum design parameter for the rotor with a straight bucket. Placing circular flat plates on the blade tips of Savonius turbines due to tip losses is positive in terms of performance. There are many studies on endplate in the literature. Looking at these studies, usage of endplate showed an increase in the coefficient of performance [15,16]. Mohamed et al. [17] defined the stator optimum point of a conventional plate.

This paper aims to increase the efficiency of Savonius wind turbine energy systems therefore the theoretical interpretations about efficiency are examined in detail. After designing model in CAD program (Solidworks), a 3D printer was also used to produce, and numerical analyzes were carried out using the Ansys Fluent program. Numerical analysis of pressure and velocity contours of Savonius wind turbines was presented in the results and discussion section. The coefficient of performance or also called as  $C_p$  ratio is obtained by the division of airflow power in turbines over the mechanical power generated by airflow. Moreover, the TSR (tip speed ratio) value which is the ratio of the linear speed of the turbine caused by its angular speed to the linear airflow speed was calculated by experiment results. Furthermore, the x-y graph of TSR vs  $C_p$  shows that as TSR increases  $C_p$  also increases exponentially at first. Then, it reaches an optimum value and after that peak point, it starts to decrease exponentially. The peak point of this graph which is called as optimum value is the maximum efficiency point of the system.

## 2. MATERIALS AND METHODS

The main objective was to find a way to increase the torque in the general formula of mechanical power. The efficiency can be controlled by changing the airflow. However, the airflow speed was determined as a constant value in the experiment. Therefore, the relationship between torque and mechanical structure of turbines was examined in detail. Using constant angular speed, the change in torque was analyzed by adding different types of plates at the bottom and top of the turbine. This process was both applied numerically and experimentally. Two different types of turbine models as straight and helical were used. The relation between torque and mechanical structure of turbines was evaluated. The parameters of

functions used to calculate the efficiency of the system are explained below.

Front view area,

$$A_{front\ view} = H * d_{rotor} \quad (1)$$

where H is the turbine height.

Mechanical power,

$$P_{turbine} = (T * \omega_{turbine}) \quad (2)$$

where T is the torque and  $\omega$  is the Turbine angular velocity.

Wind power,

$$P_{wind} = (\rho A_{front\ view} V_{wind}^3) / 2 \quad (3)$$

where  $\rho$  is the density and  $V_{wind}$  is wind speed.

Tip speed ratio,

$$TSR = (\omega_{turbine} * (d_{rotor}/2) / V_{wind}) \quad (4)$$

Coefficient of performance,

$$C_p = (P_{turbine} / P_{wind}) \quad (5)$$

### 2.1 The Production of Turbines and Their Dimensions

Firstly, the turbine has 3 blades and 2 plates which were printed using a 3D printer. The infill percentage of plates is 40% and for the blades, it is 60%. Furthermore, the print bed temperature was approximately 60°C and the temperature of the nozzle was 200°C. Medium quality PLA (Polylactic acid) 3D printing filament was used. The dimensions of a final product were matching with desired values thus production was achieved successfully. The top view and dimensions were given of Model-1 (straight-bladed) in Figure 1.

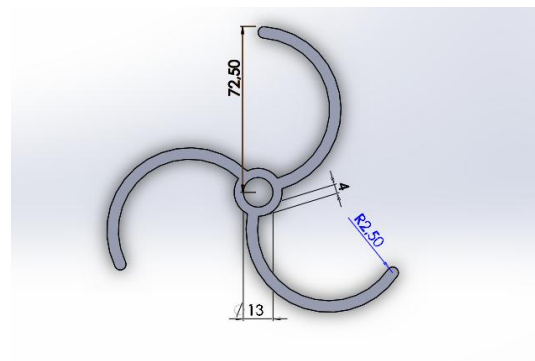


Figure 1. The Model-1 (without end plate)

Figures 3, 4, and 5 show cases where endplates are added. These plates with diameters of 5, 12, and 16 cm are indicated in figures 3, 4, and 5, respectively. The height of both models is 20 cm.

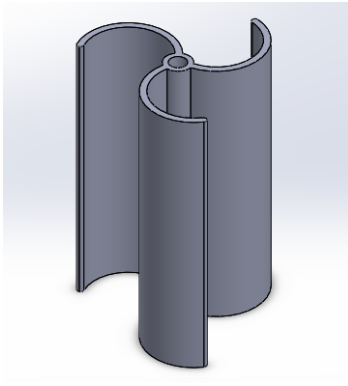


Figure 2. The Model-1 of an isometric view

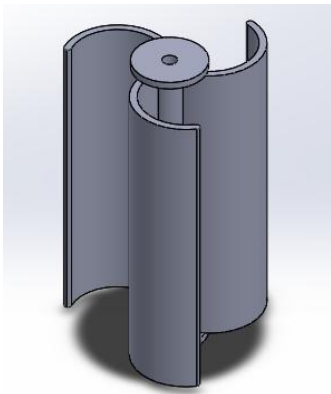


Figure 3. The Model-1 (with 5cm end plate) of an isometric view

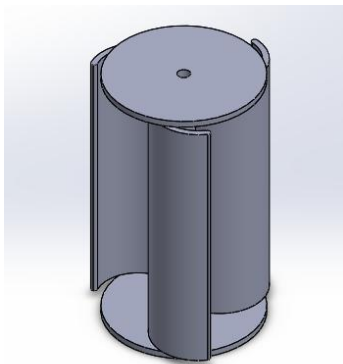


Figure 4. The Model-1 (with 12cm end plate) of an isometric view

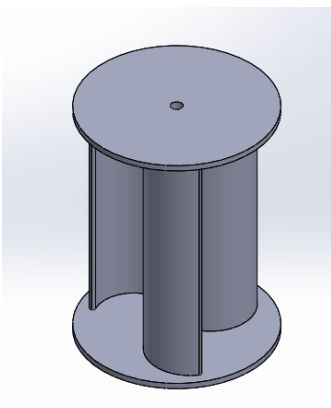


Figure 5. The Model-1 (with 16cm end plate) of an isometric view

Figure 6 indicates the general dimensions of the helical turbine. The isometric view of this turbine without an endplate can be seen in figure 7.

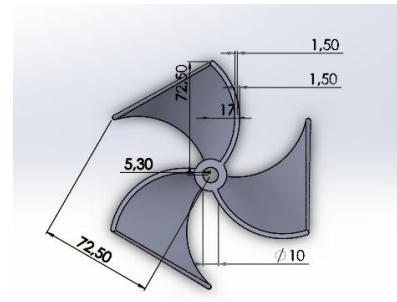


Figure 6. The Model-2 (without end plate)

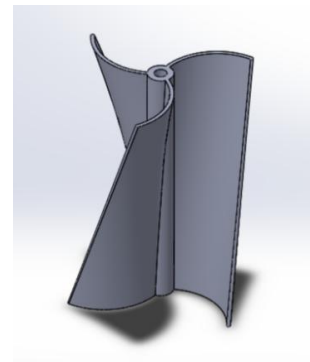


Figure 7. The Model-2 of an isometric view

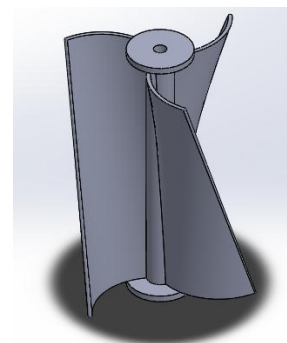


Figure 8. The Model-2 (with 5cm end plate) of an isometric view

Figures 8,9, and 10 show the state of endplates with varying diameters.

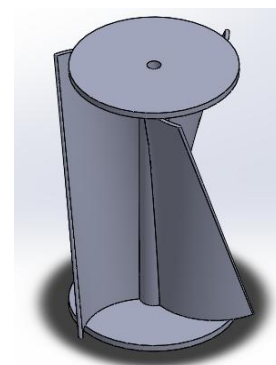
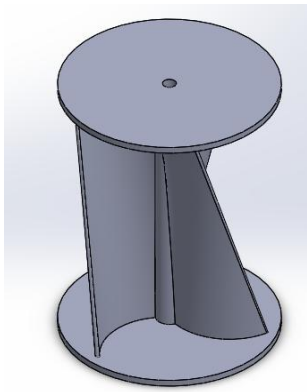


Figure 9. The Model-2 (with 12cm end plate) of an isometric view



**Figure 10.** The Model-2(with 16 cm end plate) of an isometric view

**2.2 EXPERIMENTAL ANALYSIS**

The wind tunnel is used as an experimental environment (Fig. 11 and 12).The experiment place shown in figure 11 was carried out in the aerodynamics laboratory of Erciyes University, Faculty of Aeronautics and Astronautics. Savonius wind turbines consist of one main body structure formed by 3 blades. Moreover, the values of power and efficiency were compared by applying wind tunnel tests using different types and numbers of blades. Furthermore, different-sized plates depending on the nominal diameter are placed at the bottom and top of the blades. The temperature of the experiment environment was 15°C and the dynamic viscosity value was determined as  $1.78 \times 10^{-5}$  kg/m.s based on temperature. The value of density was chosen as  $1.089 \text{ kg/m}^3$  considering the altitude. The velocity of the air inlet is constant at 10 m/s.



**Figure 11.** Photos of the wind tunnel from Aerodynamics Laboratory of Erciyes University, Faculty of Aeronautics and Astronautics

**2.2.1 Experiment Procedure**

In the experimental environment, turbines were placed in the test section of the wind tunnel. The wind tunnel has a

570x570 mm inlet and 590x590 mm outlet section at the test zone. Moreover, the airflow was supplied externally with a 15 kW electrical fan to reach the required wind speed. In order to reduce experimental errors, after the turbine started to rotate, it has waited until the voltage value produced was stabilized. Furthermore, the voltage value was reduced gradually with an electrical load and the resulting angular velocity value and torque were measured by the torque meter to the turbine shaft connected with coupling. Then, the printed end plates for the blade were mounted and the same operations were repeated. The results of the experimental analyzes made in the wind tunnel are shown in figures 13 and 14. The x-axis in these graphs is TSR (Tip Speed Ratio) and the y-axis is Cp (Coefficient of Performance). The experiment was carried out with a constant wind speed of 10 m/s, and the models used were first carried out without end plates, and then by placing plates of 5 cm, 12 cm, and 16 cm in diameter, respectively.Using the parameters mentioned before and experiment results, the graphs shown in Figures 13 and 14 were obtained. TSR- CP diagram showed that the presence of the end plate affected positively. The increase in the diameter of the end plate resulted in a greater increase in the power coefficient CP, and at the same time, it operated at high TSR values. Differences between experimental and numerical results were thought to be due to printer calibration problems in the production of models manufactured from 3D printers [19]. According to the information obtained from the experiment, the following can be said: By taking the no plates condition of the models produced as a reference, it has been seen that the plates with a smaller diameter than the nominal diameter of the models do not affect increasing the efficiency (5cm and 12cm end plates). However, positive results were obtained for the plates with a diameter larger than the nominal diameter of the models (16cm end plates) to increase the overall efficiency.

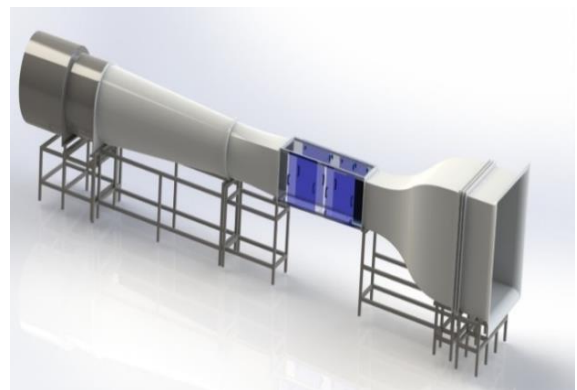


**Figure 12.**The model of the wind tunnel (adapted from [18])

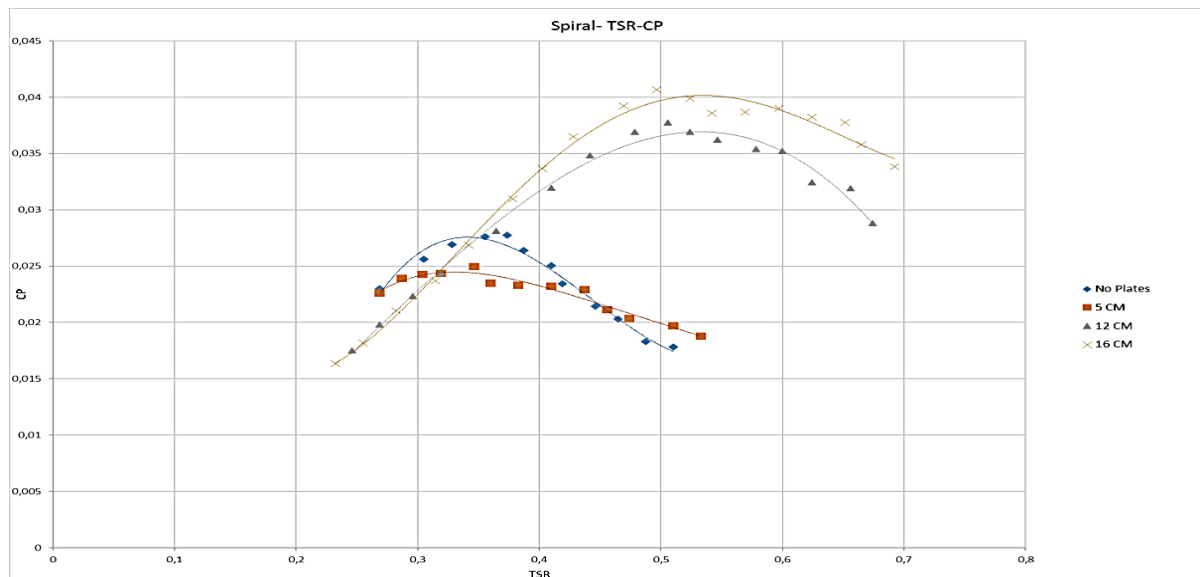


Figure 14.The Model-2 of the TSR-CP diagram

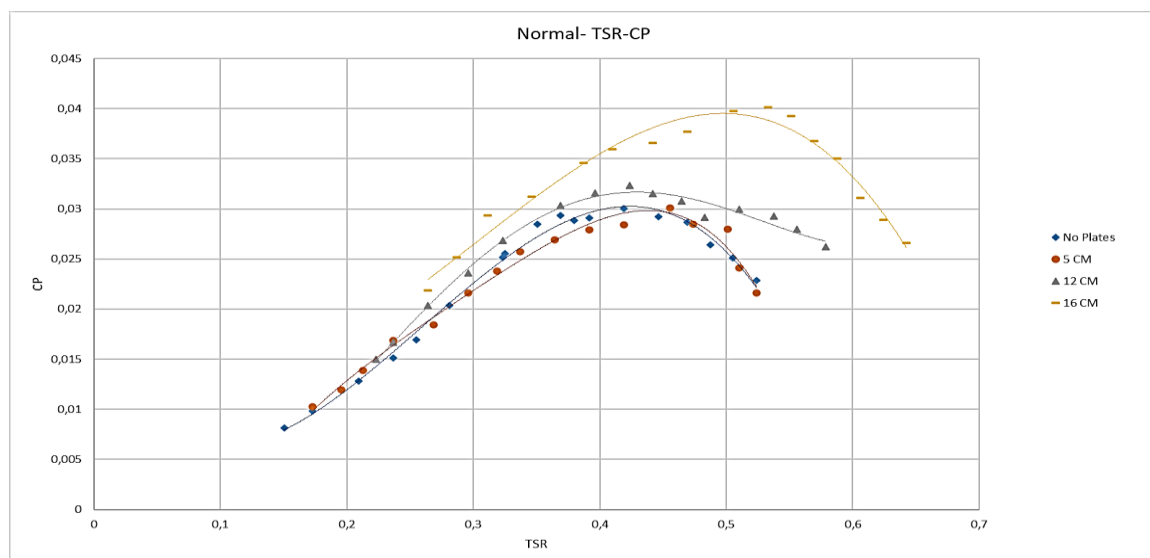


Figure 13.The Model-1 of the TSR-CP diagram

### 2.3 Numerical Analysis

ANSYS Fluent software was used to simulate the system and to compare experimental results with numerical analysis. The parameters used for numerical analysis are experimental analysis conditions. The turbulence model used for analytics has been selected as the SST  $k-\omega$  turbulence model, seen to be good at aerodynamic and turbocharger analysis in recent academic studies [1,14,20]. The SST  $k-\omega$  solving model contains both advantages of  $k-\epsilon$  and  $k-u$  turbulence models[21]. Coupled method and second-order differential solution in Fluent were chosen.

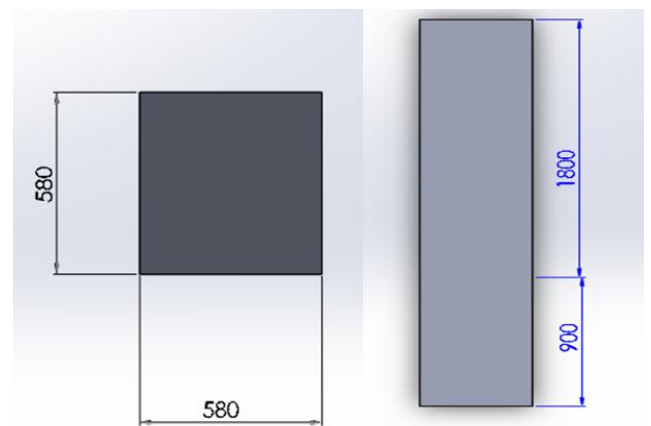


Figure 15. Size of the wind tunnel for ANSYS analysis.

In figure 15, the size of the wind tunnel was given for numerical solution. While inlet distance was 900 mm, the distance after the body was 1800 mm in length. An

isometric view of the tunnel is also given in figure 16. The cylindrical shape represents the placed turbine location which was set rotary zone.

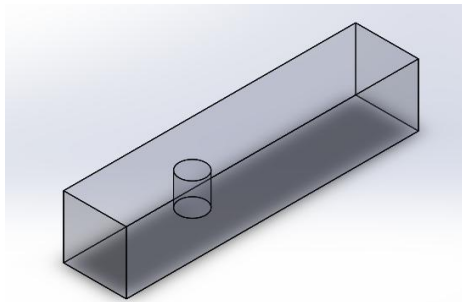


Figure 16. The wind tunnel of an isometric view

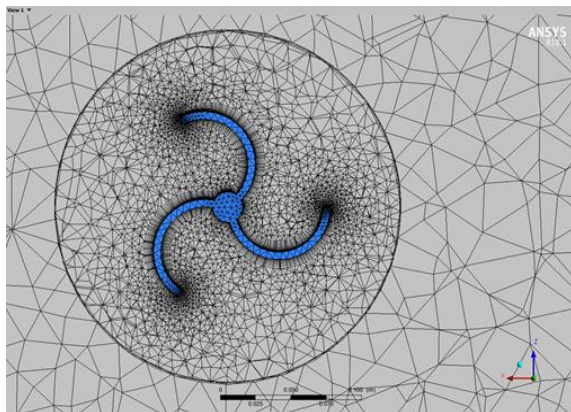


Figure 17. The Model-1's mesh structure for ANSYS analysis

Figure 17 showed a mesh structure around the Savonius wind turbine with the sectional plane.

Table 1 The table here shows only the changed settings. Settings not mentioned are taken by default in the program.

	Normal-no plates	Normal-16 cm plates added	Spiral-no plates	Spiral- 16 cm plates added
General mesh	Fine	Fine	Fine	Fine
Method	Tetrahedron (rot,tunnel) -patch conforming			
Local mesh	Sizing (wall_kanat)- 5 mm			
Inflation	Smooth transition-10 layers	Smooth transition-10 layers	Smooth transition-10 layers	Smooth transition-5 layers
Element/node statistics	1217837/361449	1300511/408196	2137710/602844	1883500/467884

A steady solution with 2000 iterations was found independent of time. The method in figure 18 was used in each analysis solution. The primary outcome in the data obtained from the analyzes here is with determining angular velocity whether the torque changes depending on different plates placed on the turbine. If the torque changes in a positive manner, that means the TSR/C<sub>p</sub> ratio mentioned above will increase. This clearly shows that maintaining more airflow within the blades provides more power output thus the efficiency increases. In addition, the analysis of the pressure and velocity distributions of the turbines was achieved with the help of CFD-post within the external flow. Therefore, it was possible to observe the airflow events and their impact around the turbine.

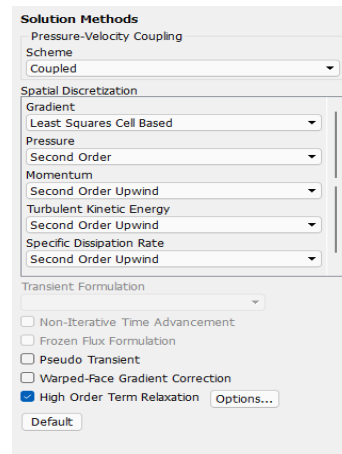


Figure 18. Solution methods

Table 2 Mesh Metric Values-Quality (Orthogonal)

Quality Values (Based On Ansys Fluent Guide)				
Name	Orthogonal Quality			
	MIN	MAX	AVG	DEVIATION
Model-1 (with no end plates)	0,11247	0,99376	0,76167	0,12237
Model-2 (with no end plates)	0,10031	0,99559	0,76156	0,11586
Model-1 (with 16 cm end plates)	0,10959	0,99561	0,75418	0,12762
Model-2 (with 16 cm end plates)	0,13315	0,99634	0,7616	0,11902

Table 3 Mesh Metric Values-Quality (Element)

Quality Values (Based On Ansys Fluent Guide)				
Name	Element Quality			
	MIN	MAX	AVG	DEVIATION
Model-1 (with no end plates)	2,0116e-002	0,99994	0,61219	0,31636
Model-2 (with no end plates)	2,1826e-002	0,99992	0,6369	0,31023
Model-1 (with 16 cm end plates)	2,2884e-002	0,99992	0,58134	0,32362
Model-2 (with 16 cm end plates)	5,5574e-002	1	0,7228	0,24058

Table 4 Mesh Metric Values-Quality (Skewness)

Quality Values (Based On Ansys Fluent Guide)				
Name	Skewness			
	MIN	MAX	AVG	DEVIATION
Model-1 (with no end plates)	1,037e-004	0,8456	0,23705	0,12256
Model-2 (with no end plates)	1,5443e-004	0,82389	0,23733	0,1165
Model-1 (with 16 cm end plates)	1,5443e-004	0,88186	0,24463	0,12787
Model-2 (with 16 cm end plates)	7,3693e-006	0,86685	0,23736	0,12045

Adequate mesh optimization could not be performed in the numerical analysis, and meshing was performed in accordance with the quality values scale found in the Ansys Fluent manual by looking at the computer capacity (tables 2, 3 and 4)[21]. The results from numerical analysis will be closer to the results of experimental analysis by using better mesh structure.

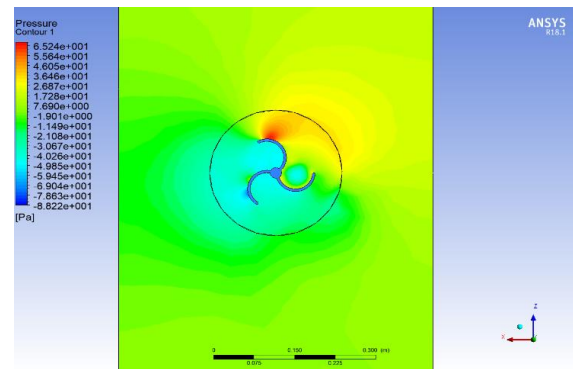
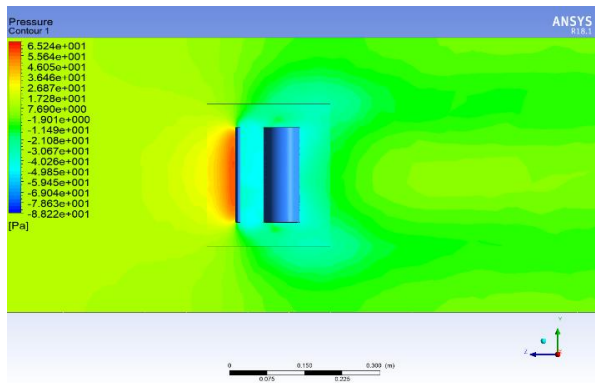
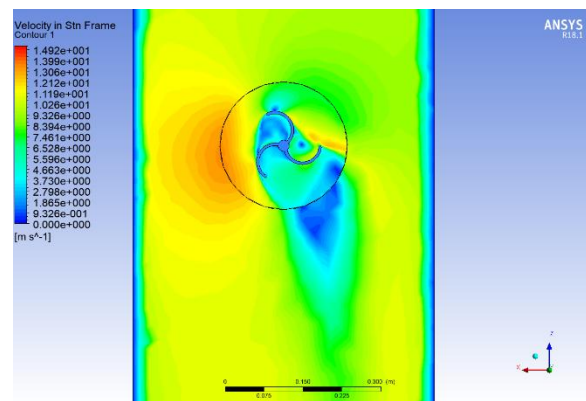


Figure 19. The Model-1's (without end plate) contour of pressure (ZX plane)



**Figure 20.** The Model-1's (without end plate) contour of pressure (YZ plane)



**Figure 21.** The Model-1's (without end plate) contour of velocity (ZX plane)

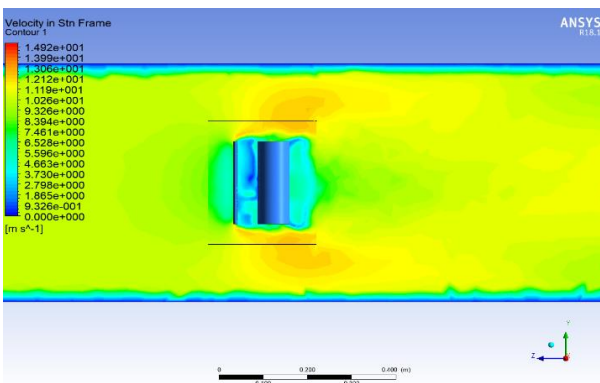


**Figure 22.** The Model-1's (without end plate) contour of velocity (YZ plane)

Bare cases of the turbine (without end plate) were demonstrated in figures 19-22. Figure 19 and figure 20 showed pressure contours, top/side view respectively. The other view defined the velocity contours. On the other hand, figures 23-26 show the same status with a diameter of 16 mm endplate. According to these figures, endplate narrowed the wake flow region and increased the speed of wind leaving the blades. The maximum pressure level did not change however pressured zone was minimized in front of the turbine.

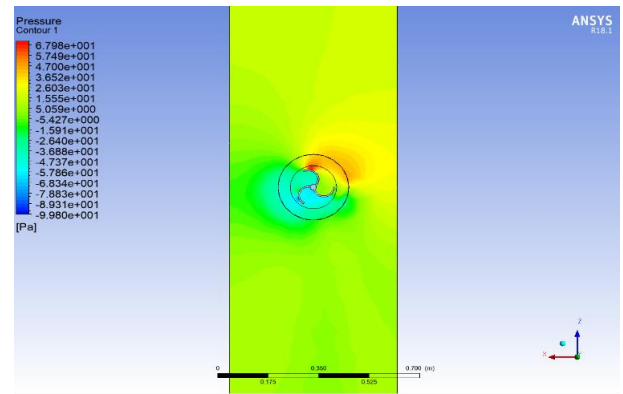


**Figure 23.** The Model-1's (with 16cm end plate) contour of pressure (ZX plane)

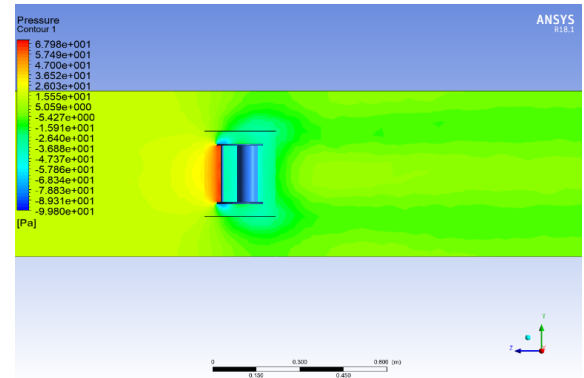


**Figure 24.** The Model-1's (with 16cm end plate) contour of pressure (YZ plane)

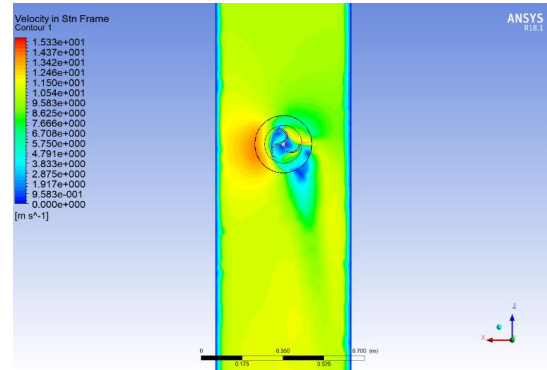


**Figure 25.** The Model-1's (with 16cm end plate) contour of velocity (ZX plane)

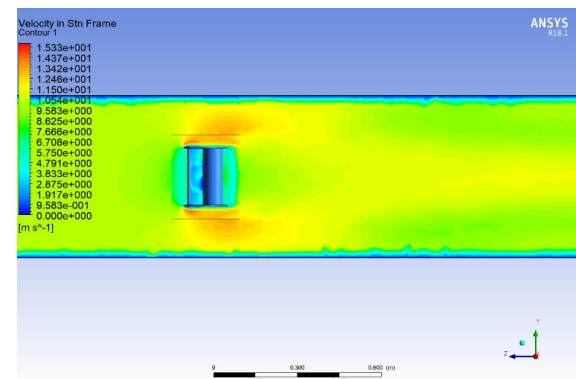


**Figure 26.** The Model-1's (with 16cm end plate) contour of velocity (YZ plane)

These figures (between 19-26) are the velocity and pressure contours created with the numerical analysis program (ANSYS Fluent CFD-post) using the data obtained from the experiments carried out in the wind tunnel. Here, figures 19-22 are the velocity and pressure contours of the analysis of the Model-1 without plates. In addition, figures (between 23-26) are the velocity and pressure contours of the model formed by placing plates with a diameter of 16 cm on the Model-1. Velocity images obtained from these areas were lower than the plated analysis of the Model-1 without plate (figures 21-22) compared to the plated analysis (figures 25- 26). The reason for this is that the Model-1 with the plate rotates faster because there is more air in the unit time structure. However, in the pressure contours obtained, it was observed that the Model-1, which was analyzed without a plated (figure 19-20), was less exposed to pressure.

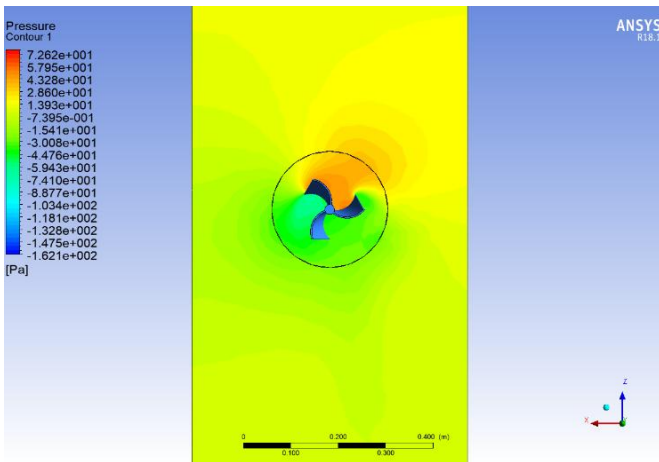


Figure 27. The Model-2's (without end plate) contour of pressure (ZX plane)

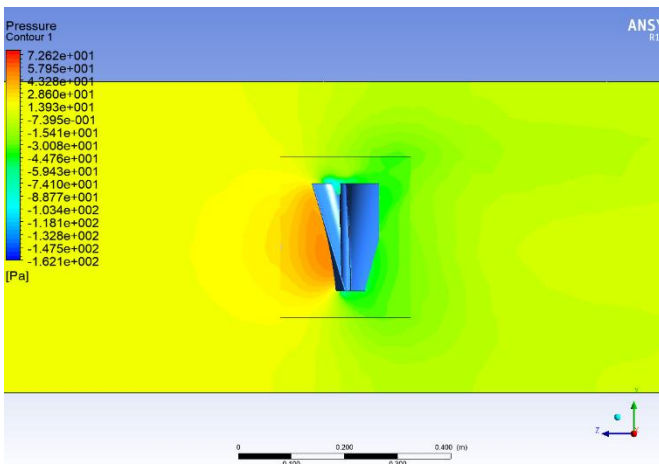


Figure 28. The Model-2's (without end plate) contour of pressure (YZ plane)

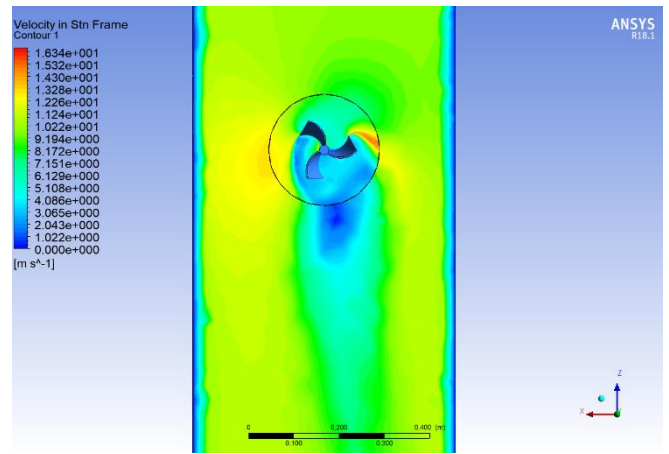


Figure 29. The Model-2's (without end plate) contour of velocity (ZX plane)

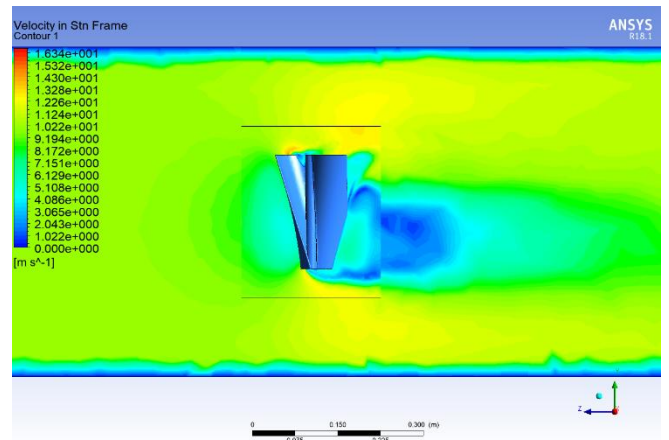


Figure 30. The Model-2's (without end plate) contour of velocity (YZ plane)

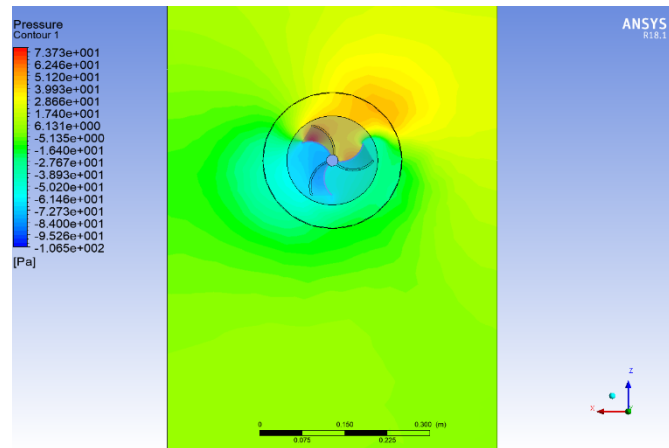


Figure 31. The Model-2's (with 16 cm end plate) contour of pressure (ZX plane)

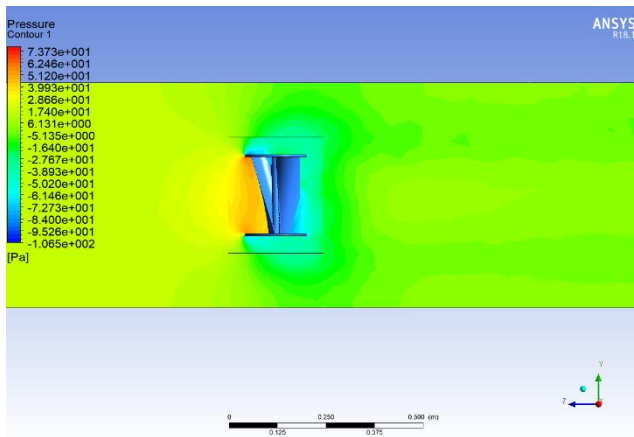


Figure 32. The Model-2's (with 16 cm end plate) contour of pressure (YZ plane)

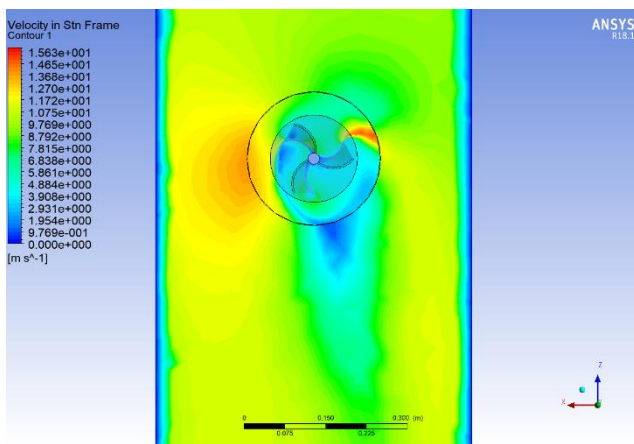


Figure 33. The Model-2's (with 16 cm end plate) velocity of pressure (ZX plane)

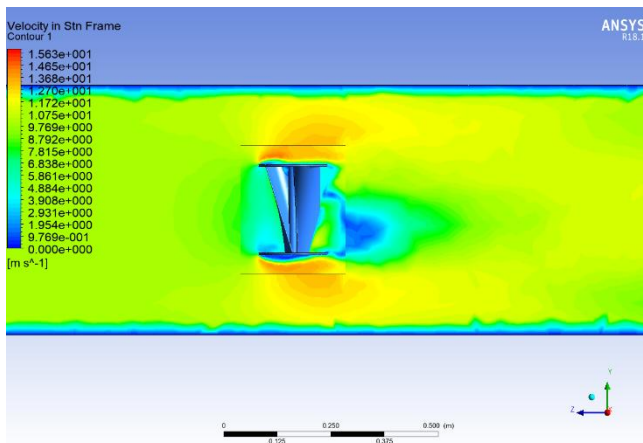


Figure 34. The Model-2's (with 16 cm end plate) velocity of pressure (YZ plane)

Here, figures 27-30 are the velocity and pressure contours of the analysis of the Model-2 without plates. In addition, figures (between 31-34) are the velocity and pressure contours of the model formed by placing plates with a diameter of 16 cm on the Model-2. Velocity images obtained from these areas were lower than the plated analysis of the Model-2 without plate (figures 29-30) compared to the plated analysis (figures 33-34). Thereason for this is that the Model-2 with the plate rotates faster due to the fact that there is more air in the blade in the unit

time structure. However, in the pressure contours obtained, it was observed that the Model-2, which was analyzed without a plated (figure 27-28), was less exposed to pressure. It is possible to see the comments made on the results of the numerical analyzes in the Model-1, similarly in the results of the numerical analyzes made in the Model-2.

Name	Experimental Data				Numerical Data				Relative Error	
	n (rpm)	T (Nm)	TSR	C <sub>p</sub>	n (rpm)	T (Nm)	TSR	C <sub>p</sub>	TSR-%	C <sub>p</sub> -%
Model-1 (with no end plates)	552	0,0082	0,4191	0,0300	552	0,0072	0,4191	0,0264	0	12
Model-2 (with no end plates)	492	0,0085	0,3735	0,0277	492	0,0155	0,3735	0,0506	0	82
Model-1 (with 16 cm end plates)	702	0,0091	0,5330	0,0402	702	0,0038	0,5330	0,0168	0	58
Model-2 (with 16 cm end plates)	654	0,0099	0,4965	0,0407	654	0,009	0,4965	0,0370	0	9

Table 5 The table here shows numerical and experimental analysis data

In table 5, 4 numerical and experimental analyses are compared. The best values that can be obtained for the design point (max c<sub>p</sub> values) should be examined both experimentally and numerically. Otherwise, it will be difficult to obtain the result because it will cause more time and cost.

### 3. RESULTS

After analyzing both the numerical analysis and the experimental data, it was concluded that when the diameter of the plates placed on the blades is larger than the nominal diameter of the models, the yield expression also increases, and when it is small, it has no positive contribution to the efficiency. In the experimental analysis, it has been observed that Model-2 with 12cm and 16cm end plates are more efficient than Model-1 with 12cm and 16cm end plates. According to the initial conditions for numerical analysis in Model-2 and Model-1, verification is performed according to max c<sub>p</sub>. the result is reliable because the data obtained from experimental analysis and data in numerical analysis are largely matched.

#### Acknowledgments

We thank Prof. Dr. Selahaddin Orhan Akansu and Merve Uzunoğlu for their assistance on this paper.

#### Nomenclatures

- T** : Torque (Nm)
- P** : Power (Watt)
- P<sub>wind</sub>** : Wind Power (Watt)
- P<sub>turbine</sub>** : Turbine Power (Watt)
- TSR** : Tip Speed Ratio (-)
- C<sub>p</sub>** : Power Coefficient (-)
- μ** : Dynamic Viscosity (kg/m.s)
- ω** : Angular Velocity (rad/s)
- ρ** : Density (kg/m<sup>3</sup>)

**REFERENCES**

- [1] Arsalan O. F. I., Numerical and experimental study with optimization of a small-scale vertical axis wind turbine, 2017. Master's Thesis. Yıldız Technical University.
- [2] Kilic F., Goktas M., Savonius Rüzgar Türbini (İkili ve Üçlü) Kanat Çevresi Akışının Sayısal Analizi. Süleyman Demirel Üniversitesi Fen Bilimleri Enstitüsü Dergisi, 2018, 22.3: 1256-1261.
- [3] Shigetomi, A.; Murai, Y.; Tasaka, Y.; Takeda, Y. Interactive flow field around two Savonius turbines. *Renew. Energy* 2011, 36, 536–545.
- [4] Sivasegaram, S. Design parameters affecting the performance of resistance-type, vertical-axis windrotors—An experimental investigation. *Wind Eng.* 1977, 1-8.
- [5] Altan, B.D.; Atılğan, M.; Özdamar, A. An experimental study on improvement of a Savonius rotor performance with curtaining. *Exp. Therm. Fluid Sci.* 2008, 32, 1673–1678.
- [6] Zhao, Z.; Zheng, Y.; Xu, X.; Liu, W. Research on the improvement of the performance of savonius rotor based on numerical study. In *Proceedings of the International Conference on Sustainable Power Generation and Supply*, Nanjing, China, 6–7 April 2009; pp. 1–6.
- [7] S. Teksin, N. Azginoglu, S.O. Akansu, Structure estimation of vertical axis wind turbine using artificial neural network, *Alexandria Engineering Journal* Volume 61, Issue 1, January 2022, Pages 305-314.
- [8] Zhao Z, Zheng Y, Xu X, Hu G. Research on the improvement of the performance of Savonius rotor based on numerical study. In: *The proceedings of the international conference on sustainable power generation and supply*; 2009. p. 1-6.
- [9] Fujisawa, N. On the torque mechanism of Savonius rotors. *J. Wind Eng. Ind. Aerodyn.* **1992**, 40, 277–292.
- [10] Gupta, R.; Biswas, A.; Sharma, K.K. Comparative study of a three-bucket Savonius rotor with a combined three-bucket Savonius-three-bladed Darrieus rotor. *Renew. Energy* 2008, 33, 1974–1981.
- [11] Simsek A., Akansu S.O, Akansu Y.A., Teksin S., Performance Analysis of Savonius Wind Turbines In Different Models, *Wind Engineering*, 2022
- [12] Lee, J.H.; Lee, Y.T.; Lim, H.C. Effect of twist angle on the performance of Savonius wind turbine. *Renew. Energy* 2016, 89, 231–244.
- [13] Akwa JV, Vielmo HA, Petry AP. A Review on the performance of Savonius wind turbines. *Renew Sustain Energy Rev* 2012;16(5):3054-64.
- [14] Menter FR. Two equations eddy-viscosity turbulence models for engineering. *AIAA J* 1994;32:1598-605.
- [15] Jeon KS, Jeong JI, Pan JK, Ryu KW. Effects of end plates with various shapes and sizes on helical Savonius wind turbines. *Renew Energy* 2015;79:167-76.
- [16] Jeon KS, Jeong JI, Pan JK, Ryu KW. Effects of end plates with various shapes and sizes on helical Savonius wind turbines. *Renew Energy* 2015;79(1):167–76.
- [17] Mohamed MH, Janiga G, Pap E, Thevenin D. Optimization of Savonius turbines using an obstacle shielding the returning blade. *Renew Energy* 2010;35(11): 2618-26.
- [18] YILMAZ, İlker, et al. Farklı Rüzgar Türbin Kanat Profillerinin Aerodinamik Performansının Deneysel İncelenmesi. *Politeknik Dergisi*, 2016, 19.4: 577-584.
- [19] ÖZDEN, Mustafa, et al. Rüzgar türbin kanadında akış kaynaklı deformasyonlarının sayısal ve deneysel incelenmesi. 3. İzmir Rüzgâr Sempozyumu, 2015.
- [20] Saad El-Deen AE, Nawar MAA, Attai YA, Abd El-Maksoud RM. On the enhancement of Savonius Bach-type rotor performance by studying the optimum stator configuration. *Ocean Eng* 2020;217:107954.
- [21] ANSYS fluent theory guide release 15.0. ANSYS, Inc.; 2013.